A Reflector Based Digital Beamforming Demonstrator

Sigurd Huber, German Aerospace Center (DLR), sigurd.huber@dlr.de, Germany
Tobias Rommel, German Aerospace Center (DLR), tobias.rommel@dlr.de, Germany
Anton Patyuchenko, German Aerospace Center (DLR), anton.patyuchenko@dlr.de, Germany
Piotr Laskowski, German Aerospace Center (DLR), piotr.laskowski@dlr.de, Germany

Abstract

In recent years a rapid development in spaceborne SAR technology can be observed. This development is driven by a wide variety of applications like the generation of highly accurate digital elevation models, the measurement of Earth surface deformation and others, with simultaneously high spatial and temporal resolution. Especially the demand of high resolution SAR imagery challenges engineers to use available technology to full capacity. An antenna concept which finds more and more promotion in the SAR community are array-fed unfoldable mesh reflectors. This concept is supplemented by a trend towards digital radars, where the signal is brought to the discrete domain almost immediately after reception. This allows for new powerful SAR modes, exceeding present-day SAR overall capabilities in terms of sensitivity, resolution and swath width by two orders of magnitude. Needless to say that such innovative SAR sensors require a thorough investigation by means of dedicated concept studies. This paper presents first digital beamforming results with a reflector based multi-channel radar demonstrator. Emphasis is laid on the verification of selected beamforming techniques, which help to show the principal feasibility of digital multi-channel SAR systems.

1 Introduction

Spaceborne SAR systems based on large unfoldable mesh reflector antennas in conjunction with digital signal processing onboard the spacecraft represent a quantum jump in next generation Earth observation systems. A forthcoming dual-satellite SAR mission adopting this technology is Tandem-L [4, 3], dedicated to monitor Earth system dynamics. Therefore it is imperative to study the feasibility of such concepts by means of demonstrators. The demonstrator developed at the Microwaves and Radar Institute of the German Aerospace Center (DLR) is a stationary ground-based system operated in X-band. The conceptual idea was to create a design, which mimics a scaled version of a potential spaceborne reflector SAR system as close as possible.

2 The Demonstrator

The main parts of the demonstrator are the transmit and receive hardware block, with the specifications summarized in **Table 1** and the reflector combined with a linear feed array [5]. The parabolically shaped reflector with elliptic aperture is faced by eight standard gain horns, as depicted in **Figure 1**. Each gain horn represents a receive channel, whose signal is individually amplified, down converted, digitized and recorded for further processing on a personal computer. Not shown in **Figure 1** is the transmit antenna. The transmit horn antenna, is installed below the receive array and points directly to the scene to be illuminated.

(a) **(b)**

Figure 1: (a) Parabolic reflector with elliptic aperture and attached feed array. (b) Feed array comprising eight 10 dB standard gain horns spaced 4.4 cm.

parameter	value
RF frequency range	9.43 . . . 9.73 GHz
RF center frequency	9.58 GHz
LO frequency	9.375 GHz
IF center frequency	205 MHz
max. output power	15 dBm
max. ADC sampl. rate	2 GS/s per ch.
ADC resolution	10 bit
large aperture diam.	1.0 m
small aperture diam.	0.7 m
focal length	0.5 m
offset	0.35 m
number of channels	8
feed spacing	4.4 cm
polarization	hh, hv, vh, hh
height above ground	12.8 m

Table 1: Specification of the ground-based reflector DBF demonstrator in X-band configuration.

Due to the large spacing of the receive feed horns of 4.4 cm, which is dictated by the base plate dimensions of the horns (see **Figure 1b**), the mutual pattern overlap between adjacent channels is relatively small, as can be observed in **Figure 2a**. This plot shows the individ-

ual far field patterns after deflection at the reflector. The corresponding phase patterns are presented in **Figure 2b**, where the phases in the mainlobe region above a minimum gain of 15 dB are shown.

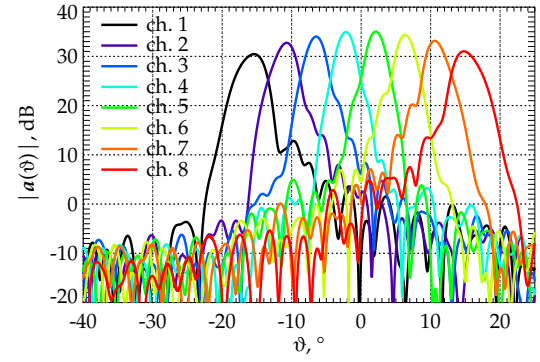

(a)

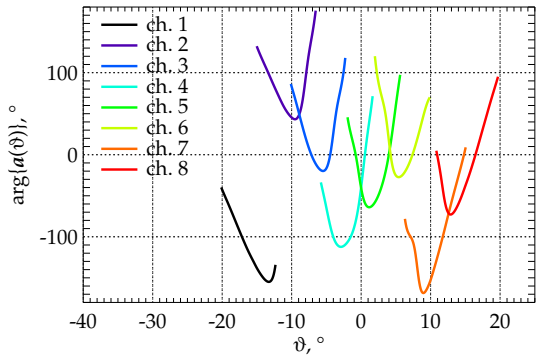

(b)

Figure 2: (a) Principal H-cut of the vv co-polar channel patterns, measured in the anechoic chamber at 9.58 GHz. (b) Corresponding phase patterns inside the mainlobe regions above a threshold of 15 dB.

Although the reflector antenna is designed such, that the symmetry plane runs through zero degree in **Figure 2**, both plots reveal a certain asymmetry, which is explained partly by imperfections in the mechanical construction process. These complex patterns have been acquired in the anechoic chamber of DLR's TechLab and serve as input for all a priori knowledge based digital beamforming experiments presented in the following. The experiments are intended to verify selected digital beamforming concepts introduced in [2] at least in their core functionalities.

2.1 Data Preprocessing

The multi-channel radar data are recorded as really sampled signals $u_{\mathrm{IF,r},i}(t)$ in the intermediate frequency (IF) band. That means in the first preprocessing step the analytic signal needs to be generated. The ith analytic channel signal $u_{\mathrm{IF},i}(t)$ is found with the Hilbert transform $\mathcal{H}\{.\}$ according to

$$u_{\mathrm{IF},i}(t) = u_{\mathrm{IF,r},i}(t) + \mathrm{j}\mathcal{H}\{u_{\mathrm{IF,r},i}(t)\} \; . \tag{1}$$

Note, the Hilbert transformer is a non-causal *infinite impulse response* (IIR) filter and has therefore to be approximated by a FIR filter. Consequently, small artifacts might be present in the analytic signal.
The second preprocessing step is the down conversion of the intermediate frequency band signal $u_{\mathrm{IF},i}(t)$ to baseband

$$u_i(t) = u_{\mathrm{IF},i}(t) \cdot \mathrm{e}^{-\mathrm{j}2\pi f_{\mathrm{IF}} t} \; . \tag{2}$$

With this, the data are available for the further digital processing.

2.2 Methods of Digital Beamforming

Having now individual data streams u_i for each individual receiver channel, the task of digital beamforming is to combine these signals to a single output u_{DBF} by means of complex weights w_i. This can be written in vector notation according to

$$u_{\mathrm{DBF}}(\boldsymbol{k}) = \boldsymbol{w}^{\mathsf{T}}(\boldsymbol{k})\boldsymbol{u}(\boldsymbol{k}) \; . \tag{3}$$

In this context the vectorial variable $\boldsymbol{k}$ represents quite generally a direction in the wavenumber space, which might be written as a function of spherical coordinates (k, φ, ϑ), $k = 2\pi/\lambda$. It is important to mention that, for a sidelooking imaging geometry, there exists a unique relation between delay time t or slant range r and the direction $\boldsymbol{k}$ under wich a certain target is seen. Finding meaningful weights is a research field by its own, known as pattern synthesis problem. Here two very basic concepts are selected, the first being a simple on- or off-switching of a specific channel. A typical weight vector would then take the form

$$\boldsymbol{w}(\boldsymbol{k}) = \begin{bmatrix} 0 & 1 & 1 & 0 & \cdots & 0 \end{bmatrix} \; . \tag{4}$$

Although very simple, this beamformer is justified by the fact that it is robust, since it requires no complex pattern information. In the following this beamformer shall be referred to as *unity* beamforming. The second beamformer can be interpreted as a spatial matched filter, which is denoted as *minimum variance distortionless response* (MVDR) beamforming [7]

$$\boldsymbol{w}^{*}(\boldsymbol{k}) = \frac{\boldsymbol{R}_{\boldsymbol{v}}^{-1}\boldsymbol{a}}{\boldsymbol{a}^{\mathsf{H}}\boldsymbol{R}_{\boldsymbol{v}}^{-1}\boldsymbol{a}} \; . \tag{5}$$

This beamformer requires knowledge of the complex array manifold $\boldsymbol{a}(\boldsymbol{k})$ and an estimate of the so called noise channel covariance matrix $\boldsymbol{R}_{\boldsymbol{v}} = \mathcal{E}\left\{\boldsymbol{v}\boldsymbol{v}^{\mathsf{H}}\right\}$.

2.3 Demonstration of DBF Principles

To verify the afore mentioned beamforming principles (4) and (5), an experiment has been conducted, for which the multi-channel radar demonstrator has been mounted on top of DLR's TechLab building as schematically indicated in **Figure 3**.

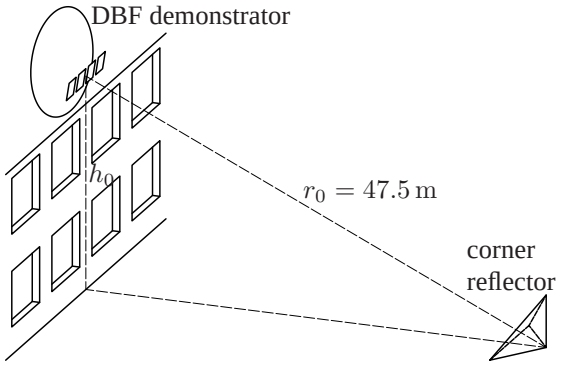

Figure 3: Simple measurement setup with a single corner reflector. The digital beamforming demonstrator is mounted on the roof of DLR's TechLab building (height $h_0 = 12.8\,\mathrm{m}$).

The reflector with feed array is aligned horizontally and pointing to the target object, a corner reflector. The corner reflector has been placed on ground in a distance of $r_0 = 47.5\,\mathrm{m}$ such, that it is seen under the horizontal angle $\vartheta = 0\,^\circ$ between channel patterns four and five (see **Figure 2**). The placement in the intersection of two adjacent channel patterns shall guarantee the largest benefit with digital beamforming in terms of gain or SNR, respectively. Ideally this gain improvement should be roughly 3 dB for MVDR beamforming, since all other channels will not contribute significantly.

For this basic experiment it proofs useful to range compress the channel signals prior to digital beamforming[1]. This method collects most of the signal energy reflected by the trihedral in a single range resolution cell of size 0.5 m, resulting in a signal with optimal SNR. The normalized range compressed channel signals $\boldsymbol{u}_{\mathrm{rc}}(r)$ as function of slant range r are shown in **Figure 4a**. Already from this plot it becomes evident that the trihedral had been placed with a slight horizontal angular offset, since the echo of the corner reflector in channel five is weaker compared to the one in channel four. The exact angular offset can be estimated using the well known *multiple signal classification* (MUSIC) algorithm [6], showing a peak at $\vartheta_0 = -0.36\,^\circ$ (see **Figure 4b**). Given the direction of arrival, the array manifold $\boldsymbol{a}$, shown in **Figure 2**, at angle ϑ_0 can be assigned to the target location in the range compressed data $\boldsymbol{u}_{\mathrm{rc}}$, depicted in **Figure 4a**, at slant range distance r_0. The performance in terms of SNR can then be evaluated at the position of the trihedral according to

$$SNR_{\boldsymbol{u}_{\mathrm{rc}}}(r_0) = \frac{|\boldsymbol{u}_{\mathrm{rc}}^{\mathsf{T}}(r_0)\boldsymbol{w}(\vartheta_0)|^2}{\boldsymbol{w}^{\mathsf{T}}(\vartheta_0)\boldsymbol{R}_{\boldsymbol{v}}(r_0)\boldsymbol{w}^{*}(\vartheta_0)} - 1\,. \qquad (6)$$

Note, the term '-1' is required since $\boldsymbol{u}_{\mathrm{rc}}$ contains signal as well as noise. As reference, for comparison purposes, also the DBF gain is computed, which can be interpreted likewise as SNR

$$SNR_{\boldsymbol{a}}(r_0) = \frac{|\boldsymbol{a}^{\mathsf{T}}(\vartheta_0)\boldsymbol{w}(\vartheta_0)|^2}{\boldsymbol{w}^{\mathsf{T}}(\vartheta_0)\boldsymbol{R}_{\boldsymbol{v}}(r_0)\boldsymbol{w}^{*}(\vartheta_0)}\,. \qquad (7)$$

The results are plotted in **Figure 5** as function of the number of activated channels N_{act} for unity as well as MVDR beamforming. Here, the SNR values have

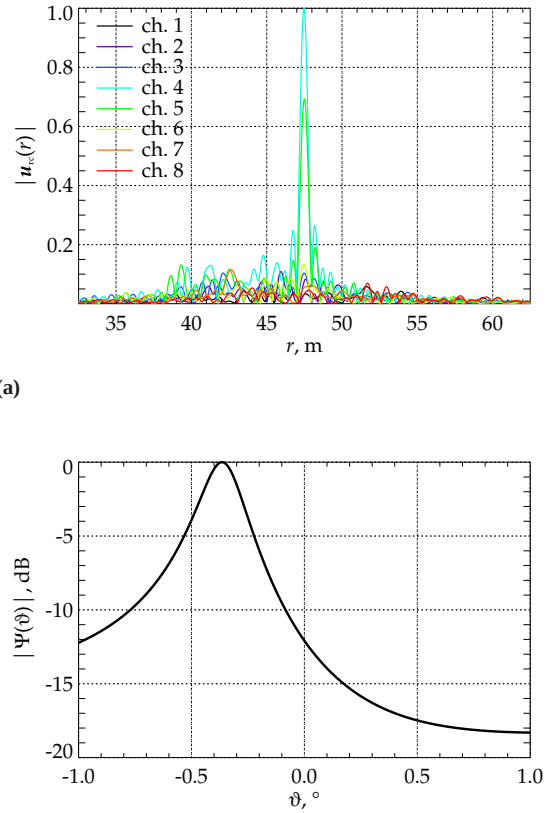

Figure 4: (a) Received signals after range compression for the individual channels. (b) MUSIC spectrum $\Psi(\vartheta)$ with a maximum at the direction of the corner reflector at $\vartheta_0 = -0.36\,^\circ$.

been normalized according to

$$\Delta SNR_{\boldsymbol{u}_{\mathrm{rc}}} = \frac{SNR_{\boldsymbol{u}_{\mathrm{rc}}}}{SNR_{\boldsymbol{u}_{\mathrm{rc}},\mathrm{MVDR}}(N_{\mathrm{act}}=1)}\,, \qquad (8)$$

$$\Delta SNR_{\boldsymbol{a}} = \frac{SNR_{\boldsymbol{a}}}{SNR_{\boldsymbol{a},\mathrm{MVDR}}(N_{\mathrm{act}}=1)}\,, \qquad (9)$$

where the respective SNR values for unity or MVDR beamforming are inserted in the numerator. The noise covariance matrices in equations (6) and (7) have been estimated from the range compressed data in far range. Here, the signal contributions are damped enough due to reflector pattern sidelobes, so that the noise only assumption holds true. A first observation in **Figure 5** is that the gain improvement with two activated channels is approximately 2 dB with MVDR beamforming. The reason for this is that the slight horizontal displacement of the trihedral caused

[1] Here the measured channel replica serve as range compression filters, performing a basic calibration of the internal signal paths of the hardware unit. Also an amplitude calibration of the range compressed signal, based on the replicas, is introduced in order to equalize channel imbalances.

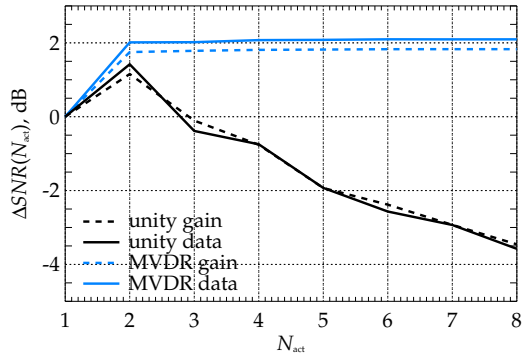

Figure 5: Relative SNR after digital beamforming at the location of the corner reflector at $r_0 = 47.5\,\mathrm{m}$ as function of the number of activated channels N_{act}.

channel five to contribute with less signal power so that the ideal improvement of 3 dB could not be reached. Unity beamforming in contrast to MVDR beamforming is a method which uses no complex pattern information. Insofar the smaller SNR value for two activated channels is explained by the fact, that the complex patterns at ϑ_0 have different phases, as can be seen in **Figure 2b**. If more than two channels are activated, the SNR for unity beamforming drops as expected, while MVDR beamforming allows to keep the SNR at a more or less constant level. This is clearly a consequence of the large feed element spacing.

3 Conclusion

This first promising demonstration example shows the potential of digital beamforming with array-fed reflector antennas. Although reflector antennas generate focused beams with relatively small overlap, it shows that MVDR beamforming is suited to improve the performance in terms of SNR especially in the overlap regions of the antenna patterns. An even larger benefit with MVDR beamforming can be achieved if defocused reflector concepts are considered [1].

References

[1] S. Huber, M. Younis, G. Krieger, and A. Moreira, "A Dual-Focus Reflector Antenna for Spaceborne SAR Systems with Digital Beamforming," *IEEE Transactions on Antennas and Propagation*, vol. 61, no. 3, pp. 1461–1465, 2013.

[2] S. Huber, M. Younis, A. Patyuchenko, G. Krieger, and A. Moreira, "Spaceborne Reflector SAR Systems with Digital Beamforming," *IEEE Transactions on Aerospace and Electronic Systems*, vol. 48, no. 4, pp. 3473–3493, Oct 2012.

[3] G. Krieger, I. Hajnsek, K. Papathanassiou, M. Eineder, M. Younis, F. D. Zan, S. Huber, P. Lopez-Dekker, P. Prats, M. Werner, Y. Shen, A. Freeman, P. Rosen, S. Hensley, B. Johnson, L. Villeux, B. Grafmüller, R. Werninghaus, R. Bamler, and A. Moreira, "Tandem-L: An Innovative Interferometric and Polarimetric SAR Mission to Monitor Earth System Dynamics with High Resolution," in *IEEE International Geoscience and Remote Sensing Symposium (IGARSS)*, Jul 2010, pp. 253–256.

[4] A. Moreira, G. Krieger, M. Younis, I. Hajnsek, K. Papathanassiou, M. Eineder, and F. D. Zan, "Tandem-L: A Mission Proposal for Monitoring Dynamic Earth Processes," in *IEEE International Geoscience and Remote Sensing Symposium (IGARSS)*, Jul 2011, pp. 1385–1388.

[5] A. Patyuchenko, T. Rommel, P. Laskowski, M. Younis, and G. Krieger, "Digital Beam-Forming Reconfigurable Radar System Demonstrator," in *IEEE International Geoscience and Remote Sensing Symposium (IGARSS)*, 2012, pp. 1541–1544.

[6] R. O. Schmidt, "Multiple Emitter Location and Signal Parameter Estimation," *IEEE Transactions on Antennas and Propagation*, vol. 34, no. 3, pp. 276–280, 1986.

[7] H. L. V. Trees, *Optimum Array Processing*. John Wiley & Sons, Inc., 2002.